2142-15

Advanced Conference on Seismic Risk Mitigation and Sustainable Development

10 - 14 May 2010

Advanced Methods of Predicting Strong Ground Motions from Crustal Earthquake Scenarios - Application to Design Basis Ground Motion for Seismic Safety of Nuclear Power Plant-

Kojiro Irikura

Kyoto University
Disaster Prevention Research Institute
Kyoto
Japan

Advanced Methods of Predicting Strong Ground Motions from Crustal Earthquake Scenarios - Application to Design Basis Ground Motion for Seismic Safety of Nuclear Power Plant-

Irikura K.(1), Kurahashi S.(2)

(1) Professor, Aichi Institute of Technology, 1247 Yachigusa, Yakusa-cho, Toyota, Aichi 470-0392, Japan, irikura@geor.or.jp
(2) Post-doctoral Fellow, ditto, susumu@aitech.ac.jp

Abstract

From recent developments of the waveform inversion analyses for rupture process using strong motion data during large earthquakes, we have understood that strong ground motions are related to slip heterogeneity inside source rather than average slip in the entire rupture area. Asperities are characterized as regions that have a large slip relative to the average slip on the rupture area, based on heterogeneous slip distributions that are estimated by the waveform inversion. We proposed a recipe for predicting strong ground motions from specific earthquakes based on the characterized source model. Verification and applicability have been examined by comparing observed ground motions with synthesized ones using the "recipe" for recent disastrous earthquakes. In this paper, first we describe the verification results for the 2007 Noto-oki earthquake. Then we apply it to simulating ground motions for the 2007 Niigata-ken Chuetsu-oki earthquake, which it happened very close to the Kasiwazaki-Kariwa Nuclear Power Plant. The active faults caused to the earthquake have not been specified for the aseismic design of the plant. Ground motions from the earthquake are found to be predictable as long as the source fault is specified through investigation of active folds and faults. Further studies are discussed to make more reliable evaluation of ground motions for earthquake safety designs.

Key-words: strong ground motion, prediction, recipe, active fault, asperity

Introduction

Importance of strong motion prediction has been widely recognized for promoting earthquake-counter measures as one of the lessons from the 1995 Kobe earthquake in Japan, The Headquarter of Earthquake Research Promotion established just after the Great Earthquake Disaster have developed "National Seismic Hazard Maps" (Earthquake Research Committee 2005). It should be more precisely called to be "Maps of Strong Motion Prediction in Japan". The maps show results of prediction of strong ground motions from two different approaches, probabilistic and deterministic, integrating survey of active faults, long-term evaluation for earthquake activities, and evaluation of strong ground motion. The probabilistic hazard maps show the probability of ground motion larger than a certain level of seismic intensity, occurring within 30 years from the present. On the other hand, the deterministic hazard maps show the ground motions (waveforms, response spectra, PGA, PGV, seismic intensity etc.) from earthquakes caused to specific active faults, based on fault models obtained from active fault surveys, historical earthquake records, and so on.

One of the problems with the probabilistic maps is that recent disastrous earthquakes have occurred in regions where probability of ground motions is relatively small, for example, the 2000 Tottori-ken Seibu earthquake (Mw 6.6-6.7), the 2004 Chuetsu earthquake (Mw 6.6), the 2005 Fukuoka-ken Seiho-oki

earthquake (Mw 6.6), the 2007 Noto-hanto earthquake (6.6-6.7), the 2007 Chuetsu-oki earthquake (6.6) and the 2008 Iwate-Miyagi-Nairiku earthquake (Mw 6.8). Therefore, the maps by themselves are not always responsible for people who expect seismologists and earthquake engineers to reduce earthquake damage for future large earthquakes. These earthquakes are caused to inland and offshore active folds and faults. A reason is that high shaking areas in probabilistic sense are related to mainly subduction earthquakes, because the probability of earthquake occurrence on the inland active folds and faults are one to two order smaller than the subduction earthquakes.

This shows that the prediction of strong ground motions from inland crustal earthquake caused to active folds and faults are required to make countermeasures for future inland earthquakes using deterministic approach, even if the probability of shaking is not so high.

The procedures of fault modeling for the prediction of strong ground motion are proposed as a "recipe" combining the active fault information with scaling relations of fault parameters from the waveform inversion of source processes using strong ground motions. We have examined the validity of the earthquake sources constructed by our recipe by comparing simulated and observed ground motions from recent inland crustal earthquakes, such as the 1995 Kobe earthquake, 2005 Fukuoka earthquake, the 2007 Noto-hanto earthquake and so on (Irikura and Miyake, 2010). Using the 'recipe' for future large earthquakes, we can provide earthquake engineers, emergency response personnel and other government and private officials with ground motion estimates that will allow them to take the appropriate action.

This technique is introduced to the "Regulatory Guide for Aseismic Design of Nuclear Power Reactor Facilities" revised in 2006 by the Nuclear Safety Commission of Japan (NSCJ, 2006).

The 2007 Niigata-ken Chuetsu-oki happened very close to the Kasiwazaki-Kariwa Nuclear Power Plant that has the largest electric output in the world. Fortunately, no severe problems have been confirmed with regard to the safety of the nuclear reactors as four of the plant's seven reactors running at the time of the earthquake were all shut down automatically by a safety mechanism according to the reports by the International Atomic Energy Agency (IAEA, 2007) as well as the Nuclear and Industrial Safety Agency in Japan (NISAJ, 2007).

There was recorded ground acceleration of 680 gals on the base mat of Unit No.1 reactor, 2.5 times more than the ground motion levels for aseismic design of facilities. The active faults caused to the earthquake have not been specified in evaluating input ground motions for the aseismic design. We need to make careful examinations why the active faults have been missed and how the ground motions have been underestimated.

In this report, we outline strong motion prediction based on the "recipe" and verification of the recipe for recent disastrous earthquakes, in particular simulations of the 2007 Chuetsu-oki earthquake.

Strong Motion Prediction Based on the "RECIPE"

The framework of strong motion prediction for crustal earthquake scenarios is shown in Fig. 1. The strong ground motions from a scenario earthquake are evaluated based on comprehensive information about (1) monitoring of seismic activity and field surveys of active faults around the target areas, (2) observation of strong ground motions, and (3) exploration of velocity structures in targeted areas. There are two important factors for predicting strong ground motion: one is source modeling for each earthquake scenario and the second is estimation of the Green's functions from source to site. Source models for specific earthquakes are derived from analysis of (1) and (2); the Green's functions are estimated using analysis of (2) and (3). Then, ground motions are predicted using the source models and the Green's functions. The validity of the results is determined by comparing the historical data with predicted motions.

Strong motions for large earthquakes are simulated, based on characterized source models defined by three kinds of parameters, outer, inner, and extra fault parameters. Those fault parameters are given by the "recipe" of strong motion prediction as shown in e.g. Irikura (2007) and Irikura and Miyake (2010).

The source model is constructed by the following procedure. First, the outer fault parameters are given as follows. Step 1: Fault Length (L) is given from geo-morphological and geological survey of active faults (Fig. 2), Fault Width (W) is estimated from of thickness of seismogenic zone and dip angle of the faults (3), and then Total Rupture Area ($S = LW$) is evaluated. Step 2: Total Seismic Moment (M_0) is given from the empirical scaling relation (Fig. 4), M_0 versus S (Irikura and Miyake, 2001). Step 3: Average Stress Drop ($\Delta\bar{\sigma}_c$) on the source fault is estimated

$$M_0 = \frac{16}{7\pi^{3/2}} \cdot \Delta\bar{\sigma}_c \cdot S^{3/2} \quad (1)$$

from the theoretical equation for circular crack model by Eshelby (1957) for aspect ratio L/W less than 2,

$$M_0 = \frac{\Delta\bar{\sigma}_c W_{max} L^2}{\alpha L + \beta} \quad (2)$$

from the equation derived by Fujii and Matsu'ura (2000) for aspect ratio more than 2. For the two constants in equation (2), are assumed $\alpha = 1.4\times10^{-2}$ and $\beta = 1.0$.

Next, the inner fault parameters are given to characterize stress heterogeneity inside the fault area. Step 4: Combined Area of Asperities (S_a) is estimated from an empirical relationship between the rupture area S as the outer fault parameter and the combined area of the asperities S_a, as the inner fault parameter as shown in Fig. 5 (Irikura and Miyake, 2001). The combined area of asperities clearly increases with the seismic moment for both inland and subduction earthquakes. The ratio S_a/S seems to be constant regardless of the rupture area with a value of about 0.22 for an inland earthquake. The stress drop on the asperities $\Delta\sigma_a$ is derived by multiplying the average stress drop over the fault $\Delta\bar{\sigma}_c$ by the ratio of the total rupture area S to the asperity area S_a (e.g., Madariaga, 1979).

$$\Delta\sigma_a = \Delta\bar{\sigma}_c \cdot \frac{S}{S_a} \quad (3)$$

Another empirical-relationship related to the inner source parameters is shown in Fig. 6. The relationship between the seismic moment M_0 and the amplitude of the acceleration source spectral level A_0 was originally found by Dan *et al.* (2001) and later confirmed by others (Morikawa and Fujiwara, 2003; Satoh, 2004).

$$A_0^a (\text{Nm/s}^2) = 2.46\times10^{10} \times (M_0(\text{Nm})\times10^7)^{1/3} \quad (4)$$

The acceleration level A_0 was theoretically related to the combined asperity areas and the stress drop in the asperities for a circular asperity by MADARIAGA (1977).

$$A_0^a = 4\sqrt{\pi}\beta v_r \Delta\sigma_a \sqrt{S_a} \quad (5)$$

The combined area of the asperities can be estimated as follows.

$$S_a = \left(\frac{7\pi^2}{4}\beta v_R\right)^2 \cdot \frac{(M_0)^2}{S\cdot(A_0^a)^2} \quad (6)$$

Step 5: Stress Drop on Asperities ($\Delta\sigma_a$) is derived as a product of $\Delta\bar{\sigma}_c$ as the outer fault parameter and S_a/S (Madariaga, 1979) from Step 4. Step 6: Number of Asperities (N) is related to the segmentation of the active faults, e.g. two per a segment. Step 7: Average Slip on Asperities (D_a) is given as $2.0\cdot D$ based on the empirical relationship by Somerville et al. (1999). Step 8: Effective Stress on Asperity (σ_α) is considered to be identical to stress drop on asperity $\Delta\sigma_\alpha$. Effective stress of background slip

areas (σ_β) is given to coincide with the average stress drop ($\Delta\bar{\sigma}_c$) over the entire rupture area. <u>Step 9: Parameterization of Slip-Velocity Time Functions</u> is given to be the Kostrov-like slip-velocity time functions as a function of peak slip-velocity and rise time based on the results of dynamic simulation by Day (1982). The peak slip-velocity is given as a function of effective stress, rupture velocity and f_{max}.

Finally, the extra fault parameters are the rupture starting point and rupture velocity to characterize the rupture propagating pattern in the fault plane. For inland crustal earthquakes, rupture nucleation and termination are related to geomorphology of active faults (e.g., Nakata et al. 1998).

This "recipe" has been applying to deterministic seismic-hazard maps for specified seismic source faults with high probability of occurrence potential in the National Seismic Hazard Maps for Japan (2005). The availability of the "recipe" has been tested in each application by the comparison between PGV's of the synthesized motions and those derived from empirical attenuation relationship by Si and Midorikawa (1999). More detailed examination for strong motion prediction should be made, comparing simulated ground motions with observed ones for recent disastrous earthquakes.

Verification of the "Recipe" for Recent Disastrous Earthquakes
We introduce two examples, one is the 2007 Noto Hanto earthquake and the other is the 2007 Niigata-ken Chuetsu-oki earthquake.

The 2007 Noto-Hanto earthquake (Mw=6.7)
This earthquake occurred west off the Noto peninsula, Japan, on March 25, 2007. Strong ground motions with the JMA seismic intensity of 6-upper struck Wajima, Anamizu, and Nanao in the northern part of the Noto peninsula. The PGA's of this earthquake with shortest fault distance seem to be a little larger than the empirical attenuation-distance relationships by Si and Midorikawa (1999) as shown in Fig. 8.

The source slip model of the 2005 Noto Hanto earthquake was determined from the inversion of strong ground motion records by Horikawa (2007) as shown in the upper left of Fig. 9. His result is not always available for strong motion simulation because the inversion is done using only long-period motions more than 1 sec. The characterized source model with asperities inside the rupture area is needed to simulate broadband motions including short-period motions less than 1 sec. for accurate estimation of seismic intensity interest. The asperities are defined as rectangular regions where the slip exceeds in the same specified manner as Somerville et al. (1999) as shown a red rectangle in the upper left of Fig. 9. For comparison, we made a source model by forward modeling, comparing between the observed records and synthesized motions based on the characterized source model using the empirical Green's function method. The best-fit source model consists of two asperities with different size shown in Fig. 10. A large one is located just above the hypocenter with an area of 6.3 x 6.3 km^2 and stress drop of about 26 MPa. A smaller one is located north-east of the large one with an area of 3.6 x 3.6 km^2 and stress drop of about 10 MPa. The stress drop of the larger asperity is about two times higher than average values of inland crustal earthquakes so far estimated.

Next, we made a source model following the "recipe" as shown in the lower right of Fig. 9, where the asperity area and stress parameters are estimated from the acceleration source spectral-level of observed data. The stress drop of the asperity estimated from the waveform inversion is almost the same as those from the recipe. However, one of the asperities by the forward modeling has a little larger stress drop (ASP1:26MPa) than the empirical ones. This result is consistent with lager acceleration than the empirical attenuation distance relation in Fig. 9. Observed motions at ISK001 and ISK003 are compared with synthesized motions for those three source models in Fig. 10. The synthesized waveforms for any models almost agree with the observed ones. Of course, the forward modeling gave the synthesized motions best-fit to the observed.

The 2007 Niigata-ken Chuetsu-oki (NCO) earthquake (Mw 6.6)

This earthquake occured on July 15, 2007 at the Niigataken Chuetsu-oki, offshore north of the Niigata-prefecture at a depth of about 17 kilometers. In the Niigata prefecture and Nagano prefecture, strong ground motions were observed as the largest intensity 6 upper. The source mechanism of this earth-

quake is supposed to be a reverse fault with the SW-NE strike and SE dip from the aftershock distribution re-determined using the OBS seismometers (ERI, Univ. of Tokyo 2008) as shown in Fig. 11. The PGA attenuation-distance relationships in Fig. 12 generally follow the empirical relations in Japan obtained by Si and Midorikawa (1999) except the KKNPP. The strong ground motions in the site of the KKNPP had markedly large accelerations more than those expected from the empirical relations. The surface motions there had the PGA of more than 1200 gals and even underground motions on one of the base-mats of the reactors locating five stories below the ground had the PGS of 680 gals. The observed records near the source area show a marked feature with three distinctive pulses in Fig. 13.

Rupture processes of this earthquake have been done by many authors using strong motion data. An example is shown in Fig, 14 (Horikawa, 2007). The slip distributions common in most of the inversion results show three asperities which generate three distinct pulses clearly seen in the observed records. However, locations of those three asperities are different each other in the source processes inverted by many authors, although almost the same data of strong ground motions were used in the analysis. The main reason why the inverted results are different is that velocity structures are too complex to assume equivalent flat-layers-structure model in calculating the Green's functions for the inversion analysis.

We attempt to simulate strong ground motions during the 2007 Niigata-ken Chuetsu-oki (NCO) earthquake based on the characterized source model. The locations of asperities are estimated by picking up the time differences between those pulses from observed records as shown in Fig.13. We find that three asperities are located south-west and south of the hypocenter in Fig. 15. In this study, we called those asperities to be ASP1, ASP2 and ASP3. We chose appropriate records of aftershocks as the empirical Green's function, taking into account locations and fault mechanisms of the aftershocks. As a result, we adopted the record of Aftershock 1 (Mw 4.4) on July 16 at 21:08 for ASP 1 and ASP2, and Aftershock 2 (Mw 3.4) on August 4 at 0:16 for ASP3. We obtained the best-fit model by forward modeling to minimize the residuals between the observed and synthesized. The areas of three asperities were about 30 km^2 and stress drop were 20 – 24 MPa.

The synthesized motions at KKZ1R2, KKZ5R2, NIG005 and NIG018 are compared with the observed ones in Fig. 17. The synthesized waveforms agree with the observed ones fairly well. In particular, three pulses appearing in the observed records at KKZ1R2 and KKZ5R2 located at B5F in underground of Unit 1 and Unit 5, respectively, are well reproduced in the synthesized velocity and displacement.

It might be likely from the viewpoint of source physics that the starting point of the ASP3 in Fig.15 is not at the edge but near the center. We find that the best-fit source model for simulating strong ground motions is available putting the starting at the upper boundary of the ASP3 as long as the propagation times from the asperity to the site are calculated with the 3-D velocity structures.

Re-evaluation of seismic safety for the Kashiwazaki-Kariwa nulclear power plant

The two earthquakes, 2007 Noto-hanto and 2007 Chuetsu-oki (NCO) earthquakes happened very close to the Nuclear Power Plants. The ground motions at the base mats of two reactors at the Shiga Nuclear Power Plant during the 2007 Noto-hanto earthquake were a little bit larger than the design spectral levels at long periods, although the facilities also have no damage. At the Kashiwazaki-Kariwa Nuclear Plant all of seven reactors were struck by strong ground motions exceeding the levels accounted for in the aseismic design of the plants. In particular, observed acceleration at the base mat of Unit 1 from the NCO earthquake was 680 gals, 2.5 times as large as the design level. Although the levels of the seismic inputs in the design of the plant were exceeded during the earthquake, "there is no visible significant damage because of the conservatisms introduced at different stages of the design process" as the IAEE report says. They also indicated that "a re-evaluation of the seismic safety for Kashiwazaki-Kariwa plant needs to be done taking account of the lessons learned from the NCO earthquake and using updated criteria and methods (IAEA, 2008)." The re-evaluation of the seismic safety should also be done for all of other nuclear power plants in Japan.

The flow of re-evaluating seismic safety of nuclear facilities as back-check based on the new regulatory guide is shown in Fig. 18. First of all, comprehensive investigation of active faults in a target area sur-

rounding the site, combining geomorphologic, geologic and geophysical surveys have been done not to miss any causative source faults. Next, advanced evaluation of the design basis ground motions (DGBM) Ss has been done by both methods, empirical response spectra and fault modeling. Further, seismic safety of important facilities and important components and piping are evaluated against the DGBM.

Concerning to the active fault surveys, there were found eight active faults and folds to be influential to the Kashiwazaki-Kariwa plant, three inland and five offshore. The largest contributions of those active faults and folds to the ground motions at the plant are from the F-B folds-band (No. 6 in Fig. 19) and from the the Nagaoka-Plain-Western-Rim fault zone connected with three faults, the Kakuta-Yahiko fault (No.1 in Fig.19), the Kihinomiya fault (No. 2 in Fig.19), and the Katakai fault (No. 3 in Fig.19) which are possibly activated together.

The DGBMs were evaluated from the F-B fault (FBF) earthquake with fault length of 36 km and the Nagaoka-Plain-Western-Rim fault (NPWRF) earthquake with that of 91 km, respectively. The acceleration time histories calculated using the fault models for the FBF earthquake and for the NPWRF earthquake are shown in Fig. 20 and Fig. 21, respectively. The fault parameters were basically given following the "recipe". The influence of uncertainties of the fault parameters on ground motions was examined, as lessons learned from the analysis of observed records from the NCO earthquake. One of them is that the stress parameters on the asperities are given to be 50 % higher than the "recipe". The ground motions with the largest responses are adopted as Ss. The ground motions from the FBF earthquake have short duration and high acceleration, while those from the NPWRF earthquake have long duration and relatively low acceleration although the NPWRF earthquake has longer fault-length and larger magnitude. The reason is that the NPWRF is located to a little further than the FBF.

The response spectra of the DBGM are shown for Unit 1 and Unit 5 in Fig. 22. The Ss-1H and Ss-3H were response spectra estimated from the empirical method for the FBF and the NPWRF, giving magnitude estimated from fault length and equivalent fault distance. The Ss-2 and the Ss-4 were calculated from the fault models for the FBF and the NPWRF. The response spectra for Unit 1 are about two times as large as those for Unit 5, reflecting the experiences of observed motions during the NCO earthquake. The difference between the Unit 1and Unit 5 sides is due to the effect of shallow underground structures to ground motions. The ground motion at the Unit 1 side was almost doubled due to the effects of the fold structure in the shallow part immediately below the site (NISA, 2008).

The S2 is the DBGM at construction time evaluated based on the old regulatory guide established in 1981. At that time, there were not found any active faults near the plant. Ground motions from a presumed event with Mj 6.5 at 10 km deep are requested to even if no active faults are detected near sited as a minimum requirement. Therefore, the main contributions to the S2 were short period motions from a presumed 6.5 earthquake with Mj located at 10 km deep and long period motions from an active fault earthquake with Mj 7.7 located at far distance of more than 100 km. The response spectra of ground motions on the free surface of the base strata estimated from the observed records of the 2007 NCO earthquake are shown by green lines. We find that the Ss were evaluated to be about two times as large as the observed ones.

The peak values of the acceleration responses of the Ss are summarized in the bottom of Fig. 22. The peak accelerations of the S2 were set to be 450 gals at the construction time. On the other hand, the Ss increased the peak values of 2300 gals for Unit 1 side including Unit 1 to Unit 4 and those of 1209 gals for Unit 5 side including Unit 5 to Unit 7. The peak values of the response accelerations at the base mats for the Ss defined at the base strata are listed in upper of Fig. 23, compared with the observed values during the NCO earthquake. It is interesting that differences between the base mats of the Units are smaller than those at the base strata, because of the effects of the shallow underground structures mentioned above. The peak accelerations on the base mats of the Units are set to be 25 % to 100 % larger than the observed ones. For example, the peak acceleration on the Unit 1 base-mat for the Ss is 845 gals, about 25 % higher than the observed value 680 gals during the NCO earthquake.

This shows that the seismic safety of the plant are enhanced much more than before as the results of re-evaluation of the seismic safety following the revision of the seismic safety regulatory guide in 2006 and the lessons learned from the 2007 Chuesu-oki earthquake.

Conclusions

Ground motions from earthquakes caused to specified source faults are evaluated using the "recipe" proposed by the scaling relations of the outer and inner fault parameters. Ground motions from the 2007 Noto-hanto (Mw 6.7) and the Niigata-ken Chuetsu-oki (NCO) earthquake are well simulated with the characterized source models based on the "recipe", as long as the source fault are specified by geomorphological and geological surveys. Uncertainties of the fault parameters make variability of about 50 % in ground motion level. Design ground motions for seismic safety are possibly estimated as long as fault modeling is appropriately made. To do that, outer and inner fault parameters should be estimated based on surveys of active faults and underground structures in propagation-path. Methodology for estimating design ground motions without specifying earthquake sources should be further improved as one of the lessons learned from the 2007 Chuetsu-oki earthquake. Source modeling based on comprehensive analysis of active faults, active folds and tectonics should be established for seismic safety design of nuclear facilities.

References

Dan, K., Watanabe, T., Sato, T. and Ishii, T. (2001), "Short-period source spectra inferred from variable-slip rupture models and modeling of earthquake fault for strong motion prediction," *Journal of Struct. Constr. Engng. AIJ,* 545, 51-62.

Day, S. M. (1982). Three-dimensional simulation of spontaneous rupture: the effect of nonuniform prestress, *Bull. Seism. Soc. Am.,* 88, 512-522.

Earthquake Research Committee (2005). Report: National Seismic Hazard Map for Japan (2005), *MEXT, http://www.jishin.go.jp/ main/ index-e.html* .

Earthquake Research Institute, Univ. of Tokyo (2008). The aftershock distribution of 2007 Chuetsu-oki earthquake re-determined using the OBS seismometers, *Report published by Earthquake Research Committee 2008,* (in Japanese).

Eshelby, J. D. (1957). The determination of the elastic field of an ellipsoidal inclusion, and related problems, *Proc. Roy Soc.,* A241, 376-396.

Fujii, Y. and Matsu'ura, M. (2000). Regional difference in scaling laws for large earthquakes and its tectonic implication, *PAGEOPH,* 157, 2283-2302.

Horikawa, H. (2007). Source rupture process of 2007 Noto-Hanto Earthquake, *http://unit.aist.go.jp/actfault/katsudo/jishin/notohanto/hakaikatei2.htm.* (in Japanese).

IAEA (2007). IAEA Mission Report : Preliminary Findings and Lessons Learned from the 16 July 2007 Earthquake at Kashiwazaki-Kariwa NPP, Vol. I., http://www.nisa.meti.go.jp/ english/index.htm.

IAEA (2008).Second Follow-up IAEA Mission in Relation to the Findings and Lessons Learned from the 16 July 2007 Earthquake at Kashiwazaki-Kariwa NPP: Vol. I., http://www.nisa.meti.go.jp/ english/index.htm.

Irikura, K. (2007). Predicting Strong Ground Motions with a "Recipe", Bull. Earthq. Res. Inst. Univ. Tokyo, 81, 341-352.

Irikura, K and S. Kurahashi (2008). Validity of Strong Motion Prediction Recipe for Inland-Crust Earthquakes, Proceedings of 14th World Conference on Earthquake Engineering October 12-17, 2008, Beijing, China, CD-Rom, Paper_ID 02-0073.

Irikura, K. and Miyake, H. (2001). Prediction of strong ground motions for scenario earthquakes, *Journal of Geography,* 110, 849-875 (in Japanese with English abstract).

Irikura, K. and H. Miyake (2002). Source modeling for strong ground motion prediction, *Chikyu, Monthly*, extra issue 37, 62-77 (in Japanese).

Irikura, K. and H. Miyake (2010). Recipe for predicting strong ground motions from crustal earthquake scenarios, Pageoph Topical Volume on "Advanced Seismic Hazard Assesment".

Kame, N. and Yamashita, T. (2003). Dynamic branching, arresting of rupture and the seismic wave radiation in self-chosen crack path modeling, *Geophys. J. Int.,* 155, 1042-1050.

Madariaga, R. (1979). On the relation between seismic moment and stress drop in the presence of stress and strength heterogeneity, *J. Geophys. Res.,* 84, 2243-2250.

Nakata, T., Shimazaki, K., Suzuki, Y. and Tsukuda, E. (1998). Fault branching and directivity of rupture propagation, *Journal of Geography,* 107, 512-528. (in Japanese).

NISAJ (2007). The Earthquakes in Niigata Prefecture and its Effects on Kashiwazaki-Kariwa Nuclear Power Station, http://www.nisa.meti.go.jp/english/index.htm.

NISAJ (2007). The Earthquakes in Niigata Prefecture and its Effects on Kashiwazaki-Kariwa Nuclear Power Station, http://www.nisa.meti.go.jp/english/index.htm.

NSCJ (2006). Regulatory Guide for Reviewing Seismic Design of Nuclear Power Reactor Facilities1, NSC Decision No. 2006-D59, Appendix 1, http://www.nsc.go.jp/NSCenglish/documents/ decisions/2006/2006_59_1.pdf.

NISAJ (2008). Kashiwazaki-Kariwa Nuclear Power Station, Tokyo Electric Power Company Interim Report on the Geology and Geological Structure of the Ground Surrounding the Site and on the Evaluation of the Design Basis Ground Motions, http://www.nisa.meti.go.jp/text/kokusai/IAEA2ndFU/ 01-G1-NISA 01_Report_Evaluation of Seismic Ground Motion.pdf (1,338,590 bytes)

Si, H. and Midorikawa, S. (1999). New attenuation relationships for peak ground acceleration and velocity considering effects of fault type and site condition, *J. Struct. Constr. Eng., AIJ.,* 523, 63-70. (in Japanese with English abstract).

Somerville, P. G., Irikura, K., Graves, R., Sawada, S., Wald, D., Abrahamson, N., Iwasaki, T., Kagawa, T., Smith, N. and Kowada, A. (1999). Characterizing crustal earthquake slip models for the prediction of strong ground motion, *Seism. Res. Lett.,* 70, 59-80.
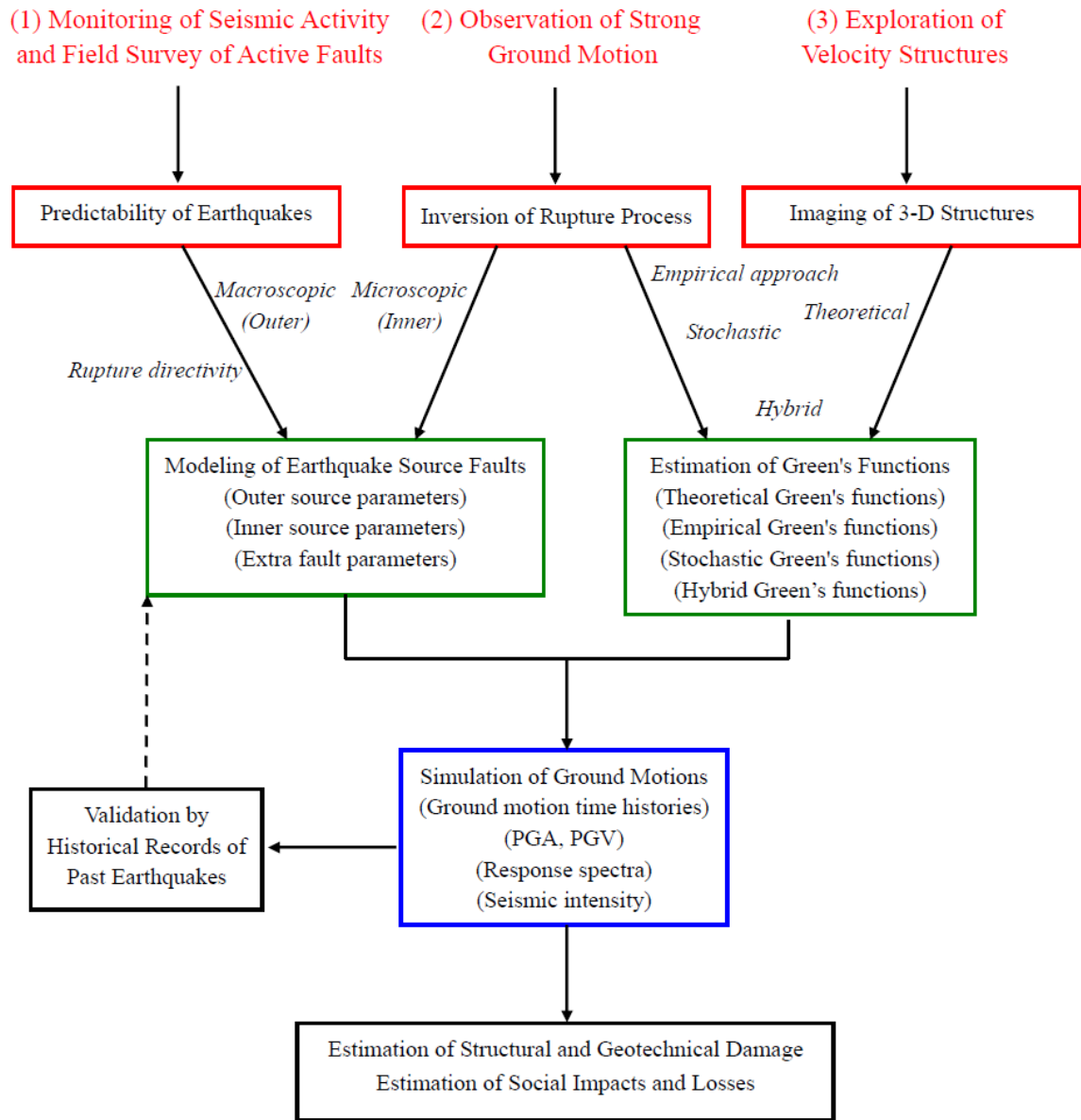
(1) Monitoring of Seismic Activity and Field Survey of Active Faults

(2) Observation of Strong Ground Motion

(3) Exploration of Velocity Structures

Predictability of Earthquakes

Inversion of Rupture Process

Imaging of 3-D Structures

Macroscopic (Outer)

Microscopic (Inner)

Rupture directivity

Empirical approach

Stochastic

Theoretical

Hybrid

Modeling of Earthquake Source Faults
(Outer source parameters)
(Inner source parameters)
(Extra fault parameters)

Estimation of Green's Functions
(Theoretical Green's functions)
(Empirical Green's functions)
(Stochastic Green's functions)
(Hybrid Green's functions)

Validation by
Historical Records of
Past Earthquakes

Simulation of Ground Motions
(Ground motion time histories)
(PGA, PGV)
(Response spectra)
(Seismic intensity)

Estimation of Structural and Geotechnical Damage
Estimation of Social Impacts and Losses

Fig. 1. Framework of predicting strong ground motions for crustal earthquake scenarios.
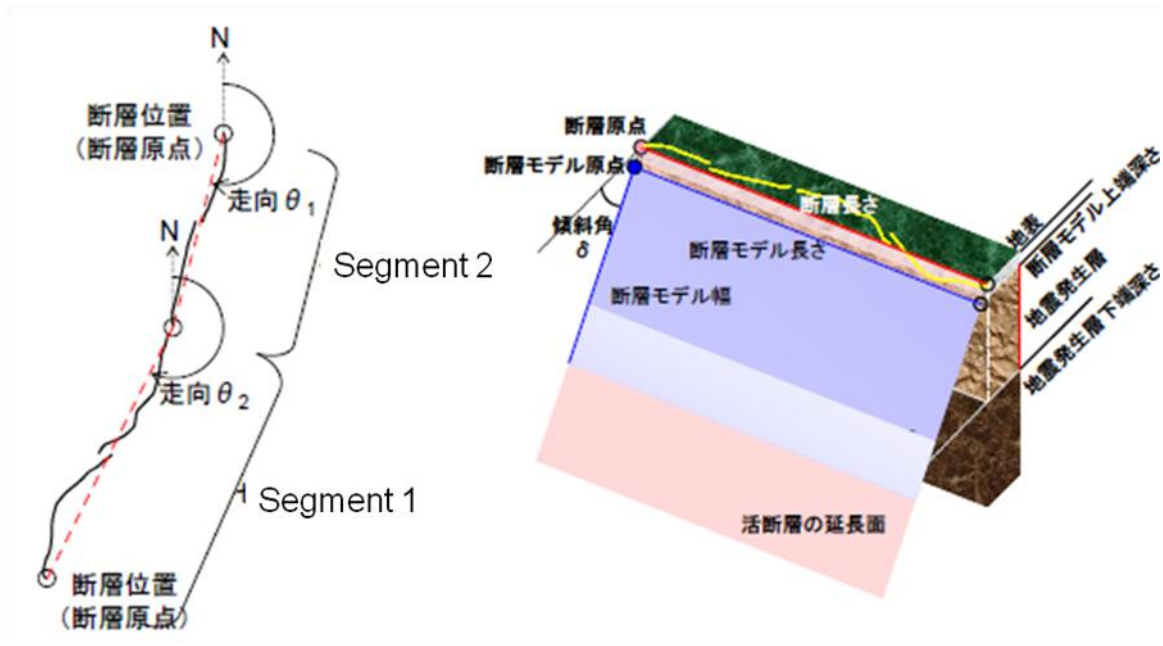
Fig. 2. Source modeling for fault length and fault width. Fault length is given to be the sum of fault segments simultaneously activated.
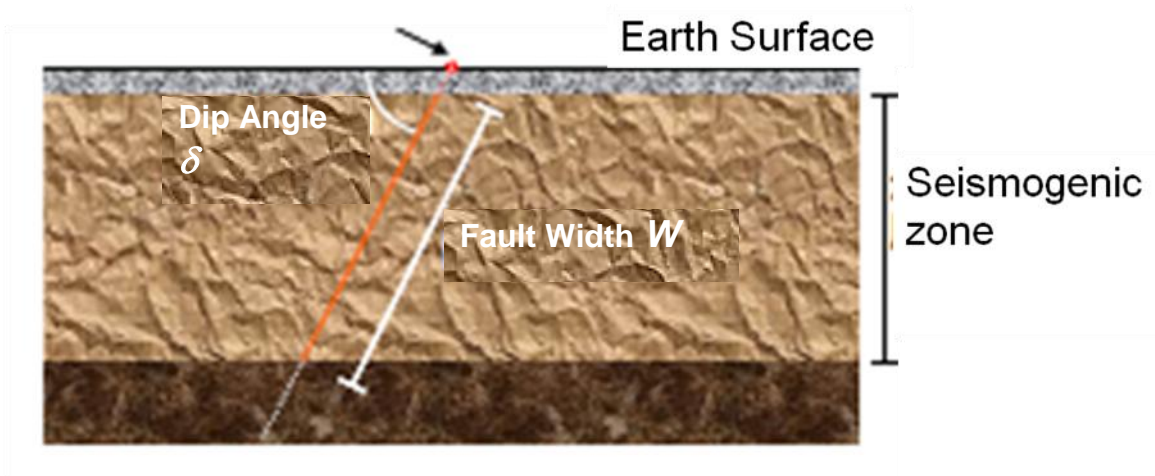
Fig. 3. Definition of fault width W. W is given to be $Hs/\cos(\delta)$ where Hs and δ are thickness of seismo-genic zone and dip angle, respectively.
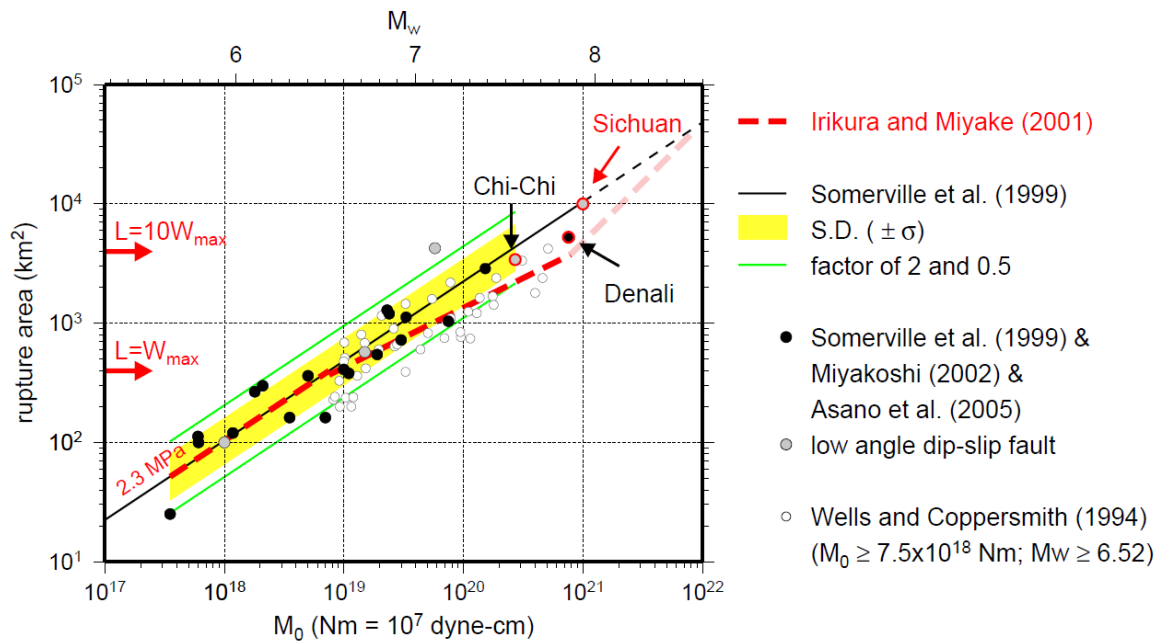
Fig. 4. Empirical relationships between seismic moment and rupture area for inland crustal earthquakes. Red broken lines are the 3-stage scaling relationships proposed by our studies (after Irikura and Miyake, 2001; Irikura *et al*., 2004).
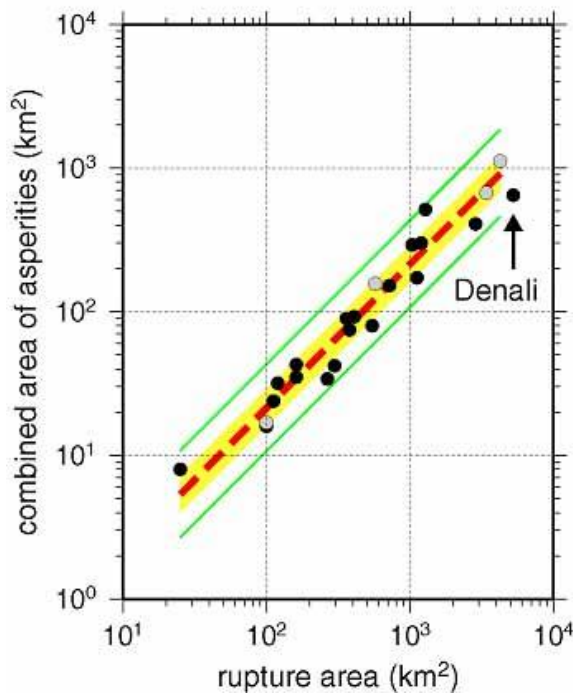
Fig. 5. Empirical relationships between combined area of asperities and total rupture area for inland crustal earthquakes (after Irikura and Miyake, 2001). Shaded areas represent $\pm\,\sigma$ (standard deviation). The thin solid lines show a factor of 2 and 1/2 for the average. The database obtained by waveform inversions is from Somerville *et al*. (1999) and Miyakoshi (2002).
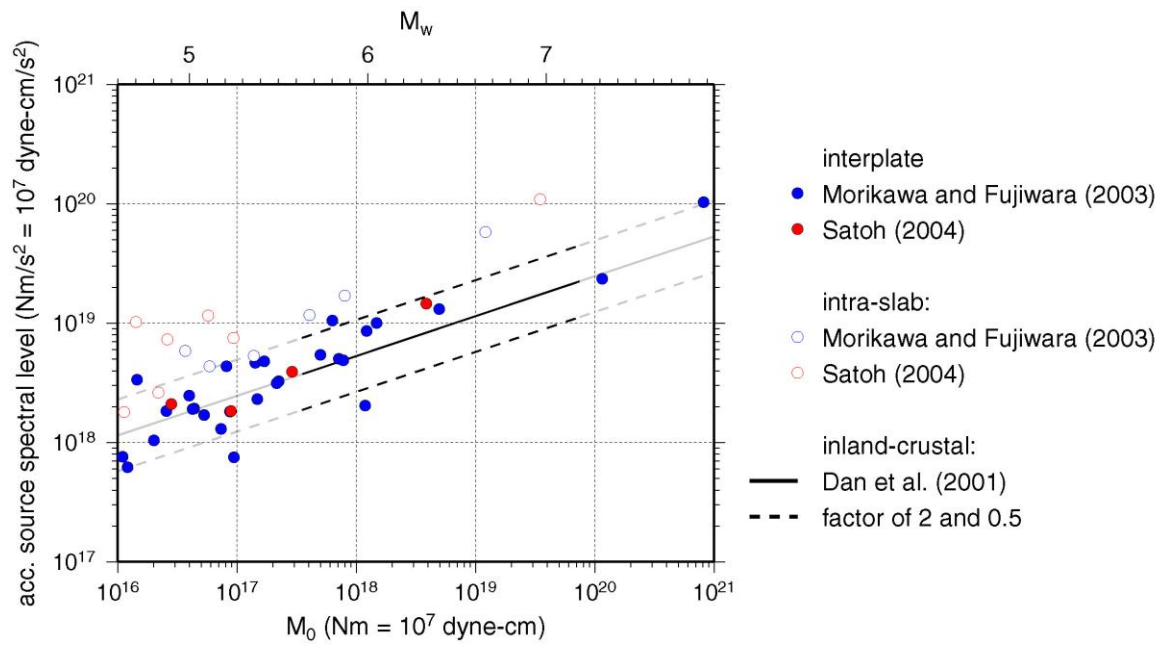
Fig. 6. Empirical relationship between seismic moment and acceleration source-spectral level.
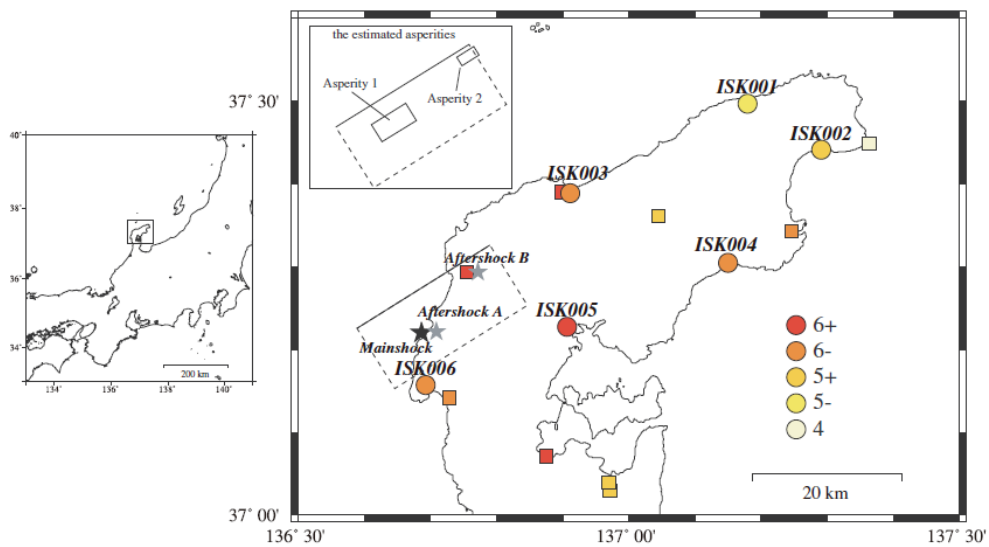
Fig. 7. Map showing source fault of 2007 Noto Hanto earthquake (rectangular), the locations of stations used for analysis (circle), the other stations (square) and epicenter of the mainshock (star).
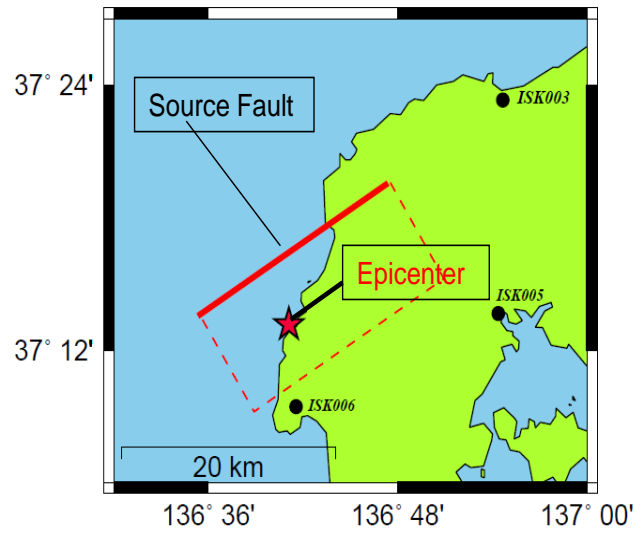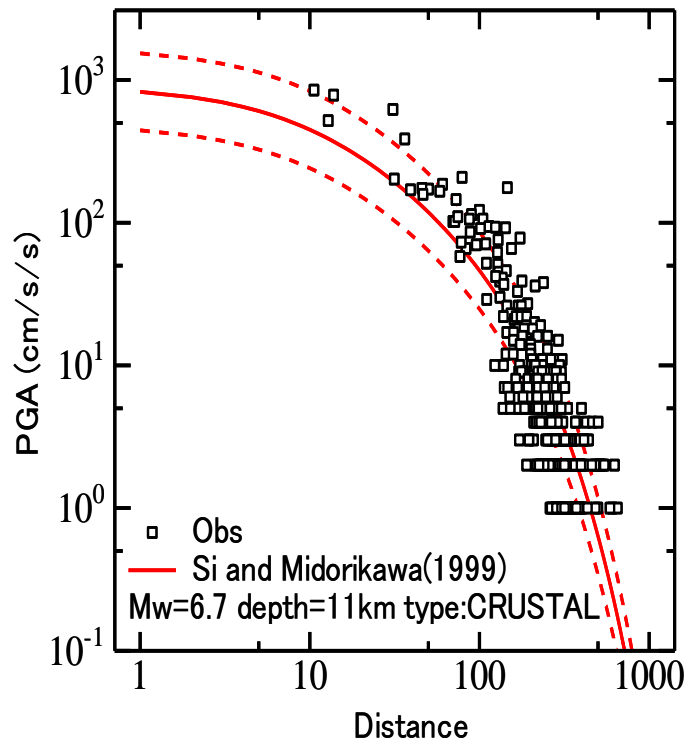
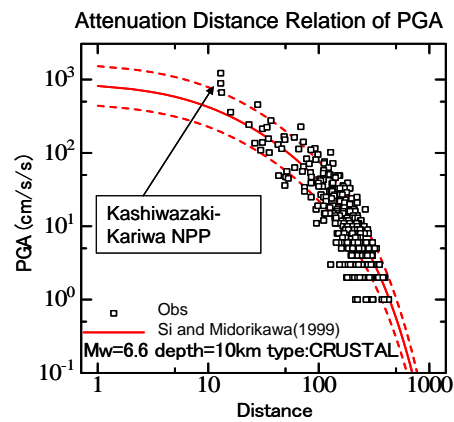Fig. 8. Upper: Map showing source fault by Horikawa (2007). Lower: Relationship of observed peak horizontal ground accelerations versus shortest distances to the source fault. Red solid and dotted curves show the empirical PGA attenuation distance relationship for surface data by Si and Midorikawa (1999) and its standard deviation (lower).
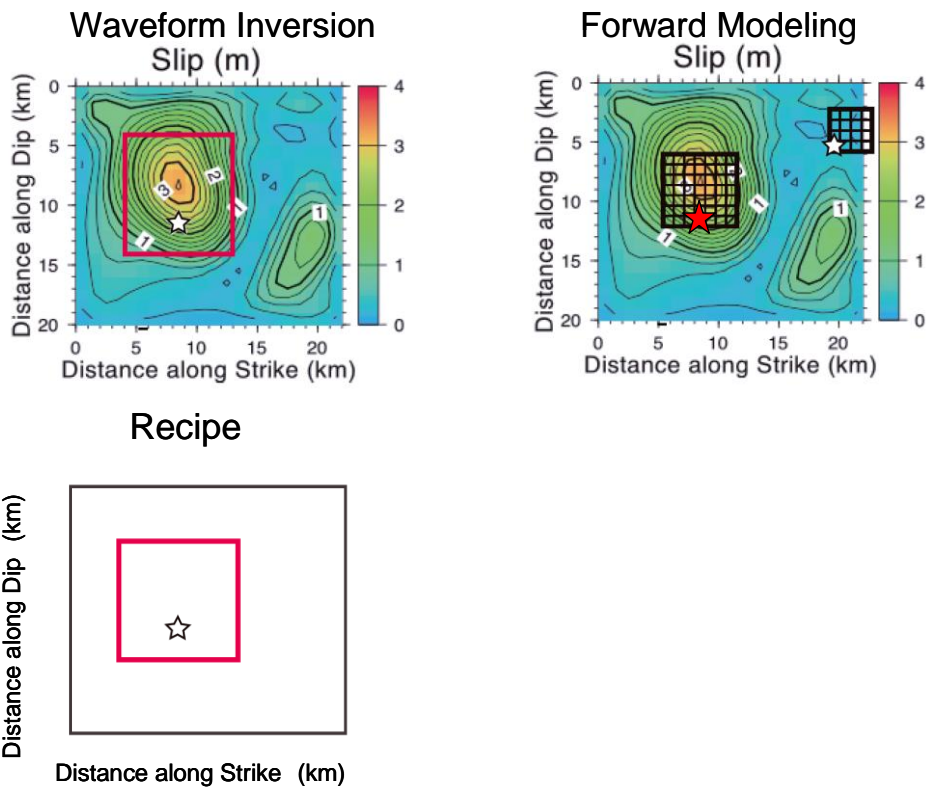
Fig. 9. Characterized source models with asperities inside the rupture area. Upper left is a model by waveform inversion result and upper right is that by forward modeling. Lower left is that by recipe.
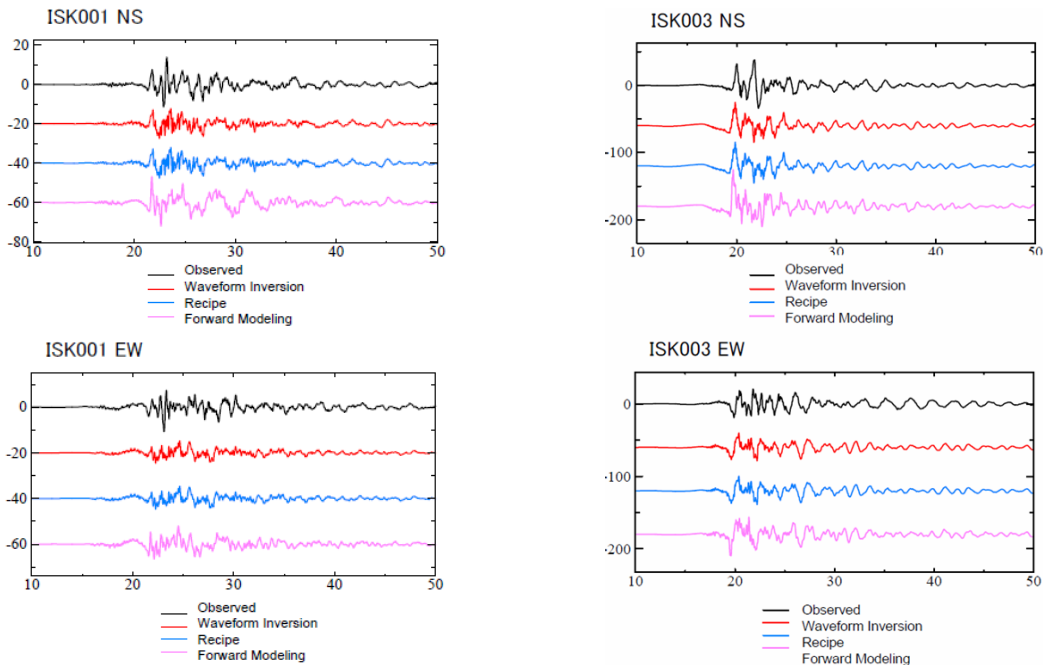
Fig. 10. Comparison between observed records and synthesized motions for three source models by waveform inversion, recipe, and forward modeling at ISK001 and ISK003.
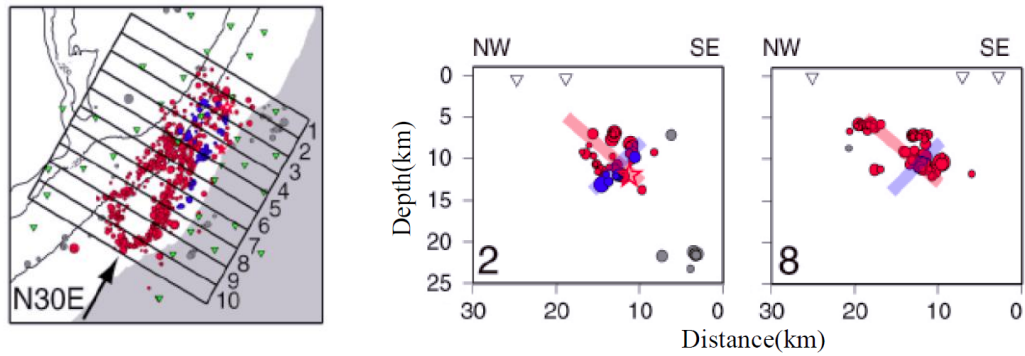
Fig. 11. Aftershock distributions in the horizontal plane (left) and cross section perpendicular to the strike (right) using the OBS seismometers (ERI, Univ. of Tokyo,2008).

Fig. 12. Relationship of observed peak horizontal ground accelerations versus shortest distances to source fault. Red solid and dotted curves show the empirical PGA attenuation distance relationship for surface data by Si and Midorikawa (1999) and its standard deviation.
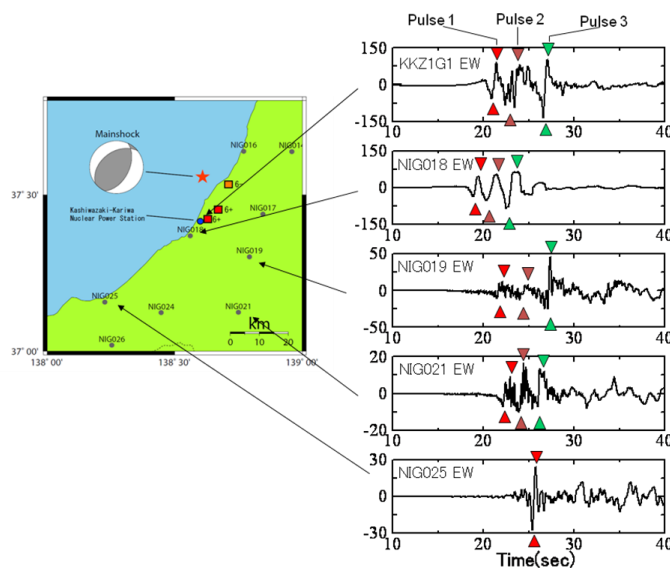

Fig. 13. Strong motion records (velocity) near the source area. The uppermost record was obtained at the surface station near Unit No.1 Reactor.
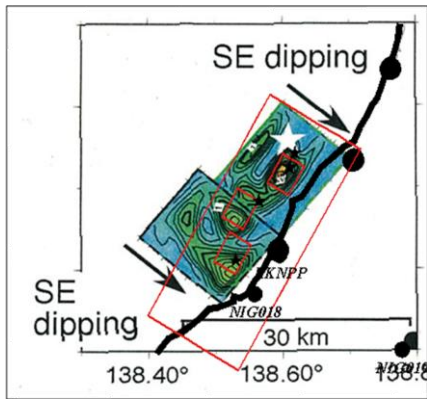
Fig.14. Slip distribution inverted the waveform inversion using strong motion data (Horikawa, 2007). Red rectangles show strong motion generation areas estimated by forward modeling in Fig. 15.
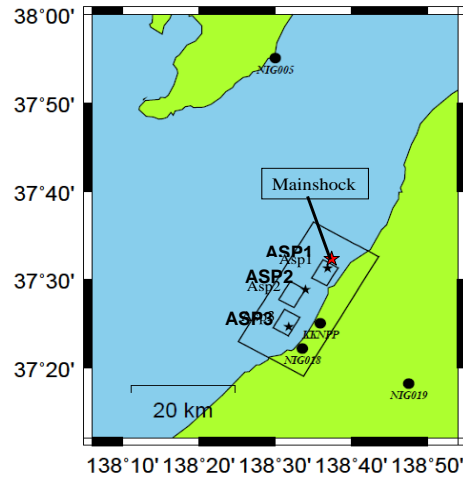

Fig. 15. Map showing source model (rectangle) consisting of three asperities (Asp1, Asp2 and Asp3) in this study and the locations of K-net stations and KKNPP (circle) and the epicenter of the mainshock (red star).
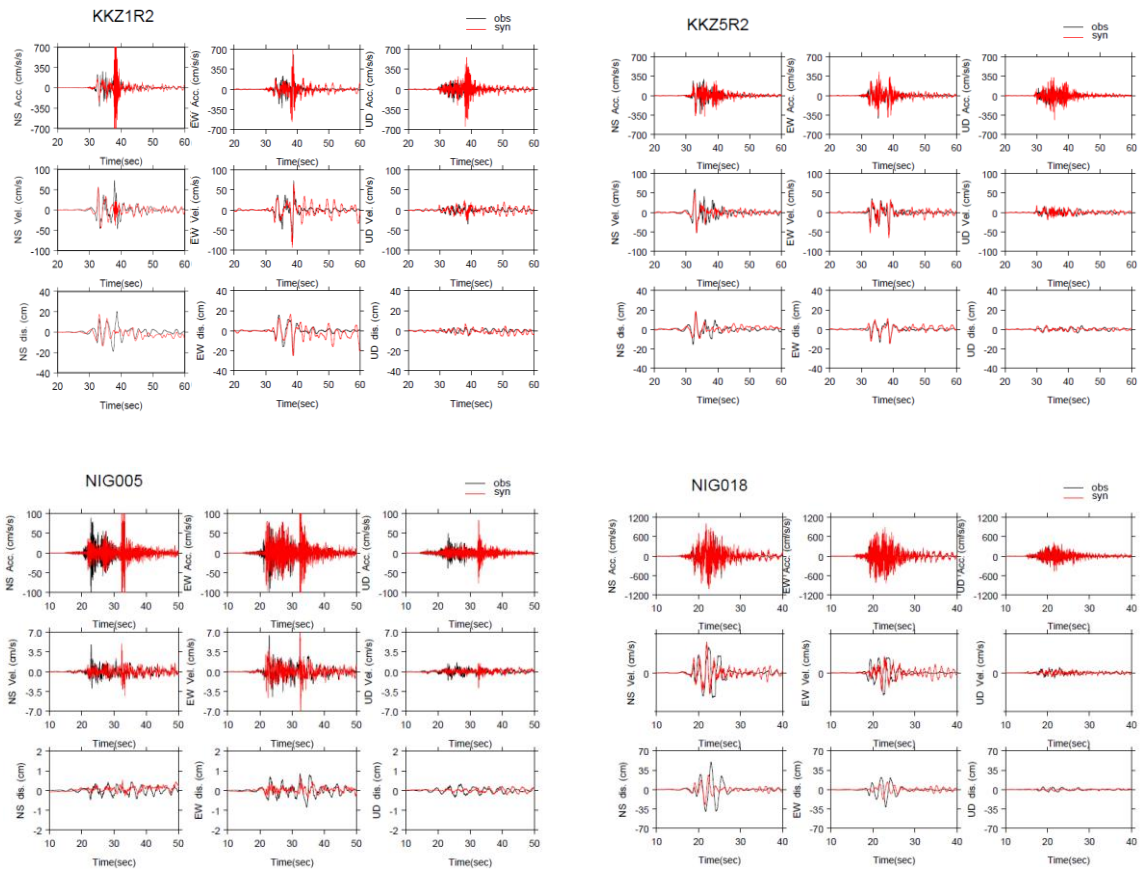

Fig. 17. Comparison between the observed records (black) and synthesized motions (red). Acceleration (top), velocity (middle) and displacement (bottom) are shown at KKZ1R2, KKZ5R2, NIG005 and NIG018.
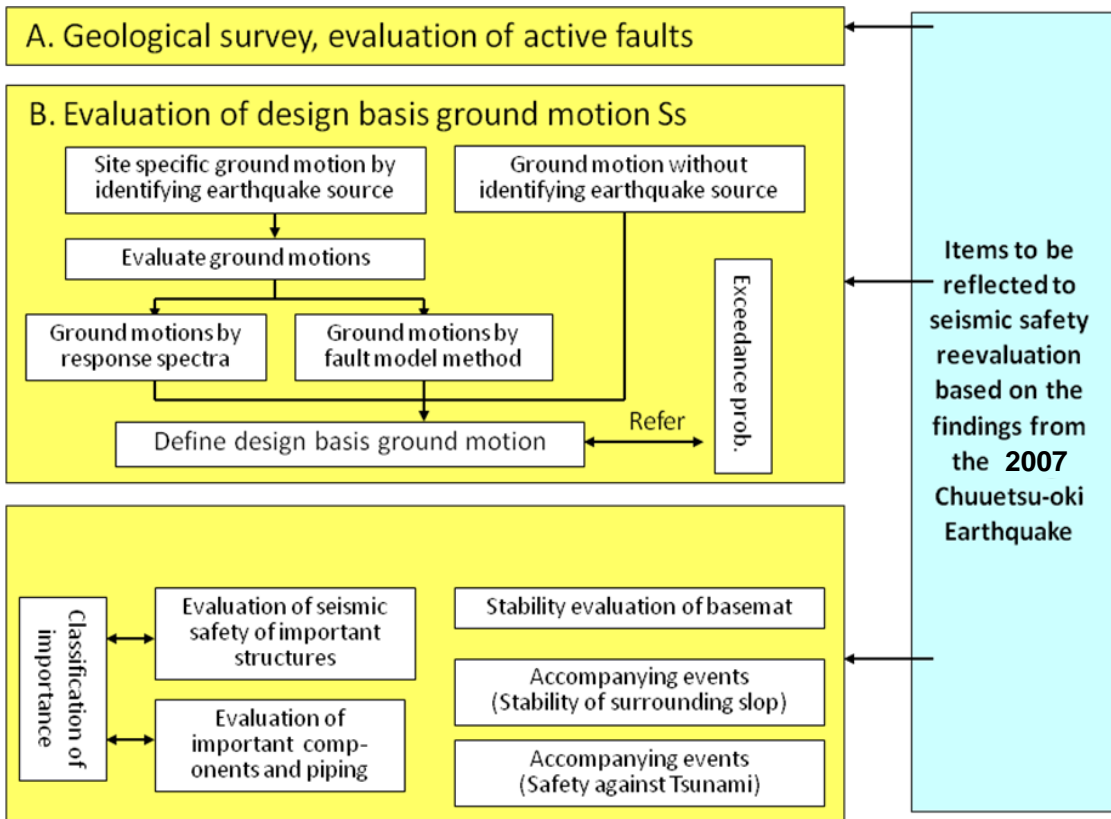
Fig. 18. Flow of reevaluating seismic safety of nuclear power plants based on the new seismic safety regulatory guide established in 2006.
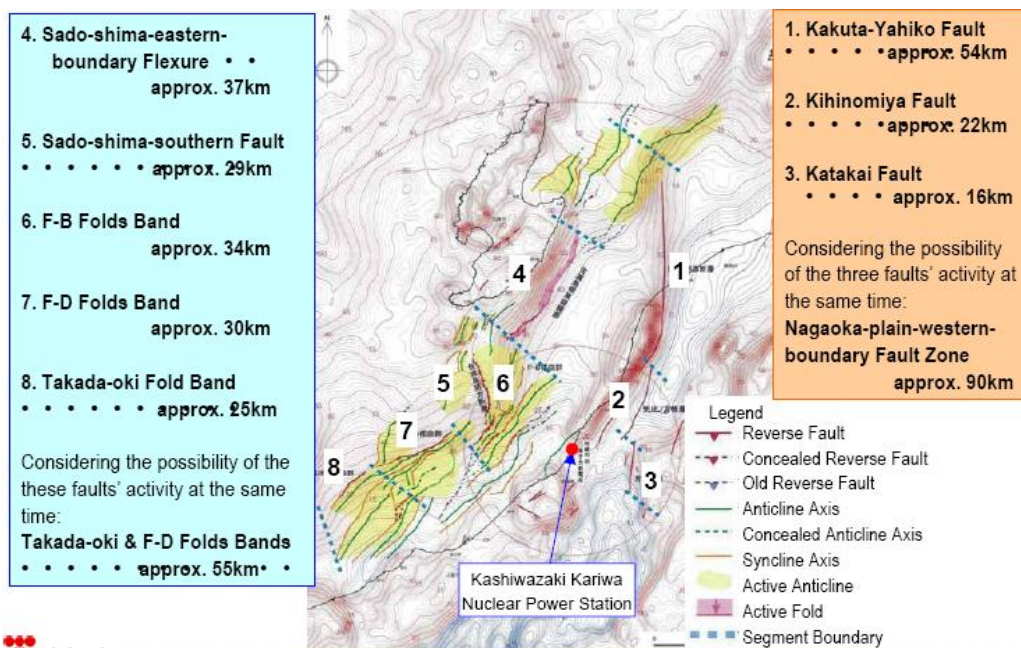

Fig. 19. Active faults and folds near the Kashiwazaki-Kariwa Nuclear Power Stations.

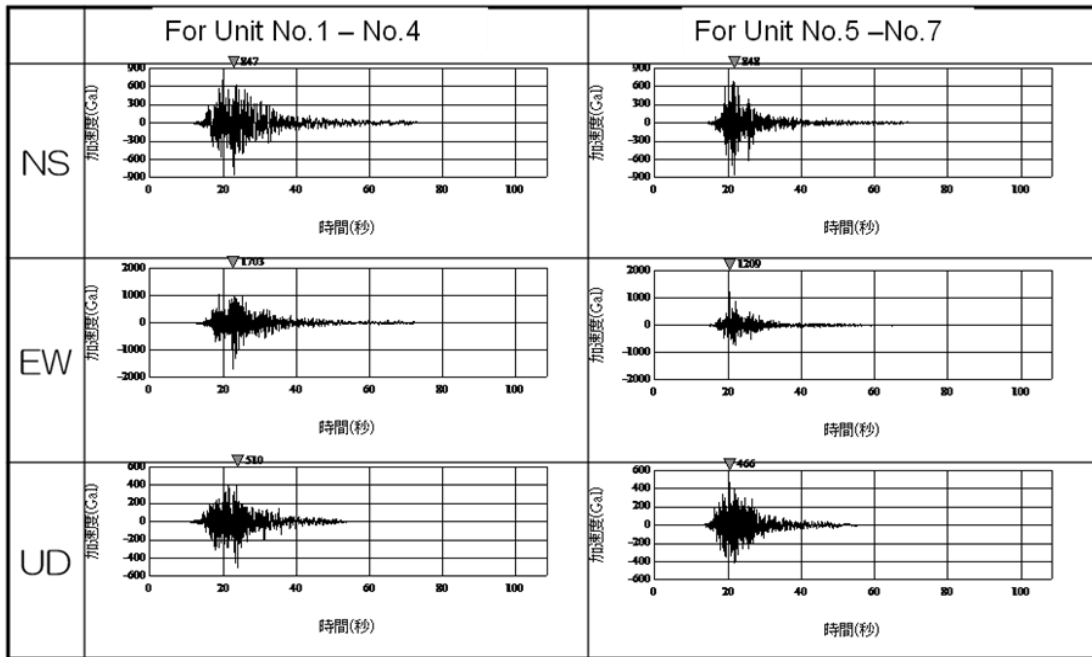**Acceleration Time Histories from the F-B Folds Band Earthquake**

Fig. 20. The design basis ground motions (DBGMs) Ss-2 evaluated using the fault model for the F-B Folds Band Earthquake. The DBGMs are defined on free surface of base strata.

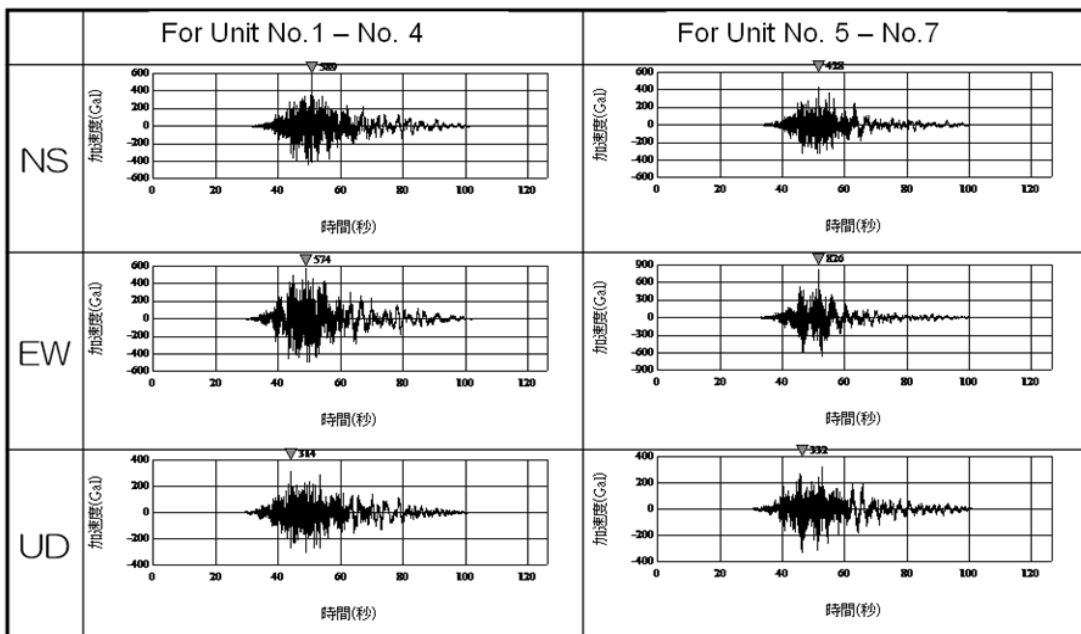**Acceleration Time Histories from the Nagaoka-Plane-Western- Rim Fault Zone Earthquake**

Fig. 21. Design Basis Ground Motions (DBGMs) Ss-3 evaluated using the fault model for the Nagaoka-Plane-Western-Rim Fault Zone Earthquake .
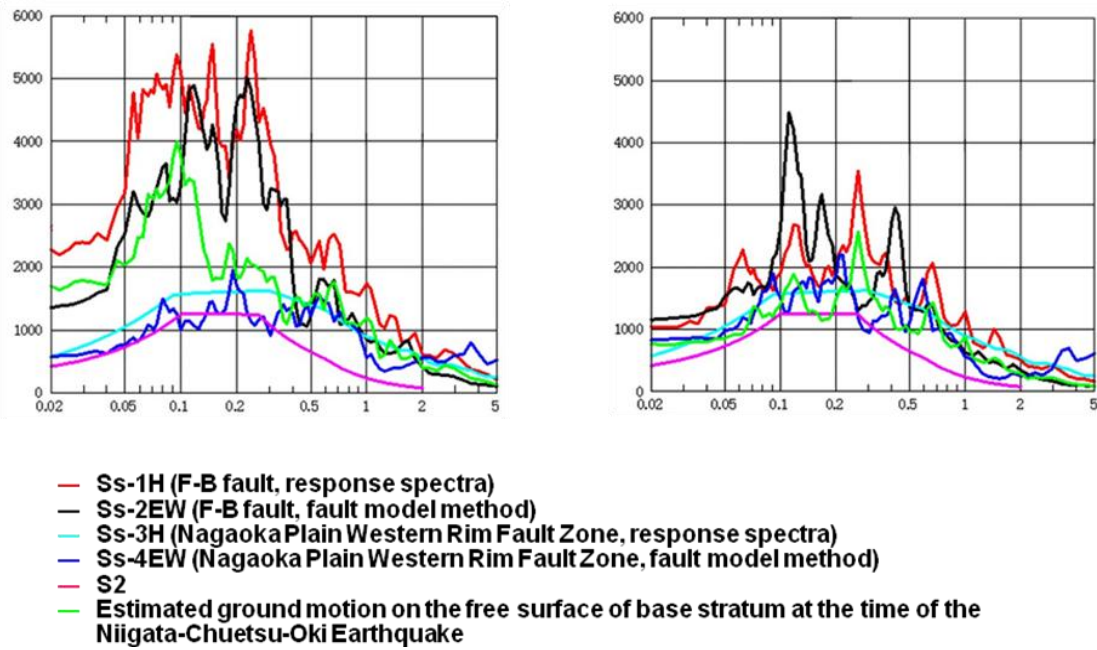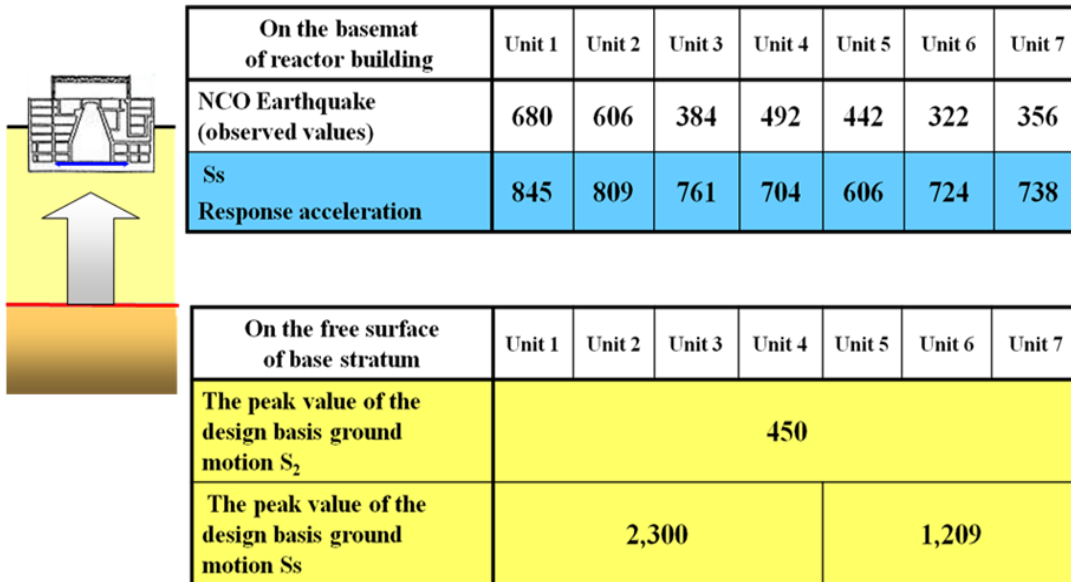
— Ss-1H (F-B fault, response spectra)
— Ss-2EW (F-B fault, fault model method)
— Ss-3H (Nagaoka Plain Western Rim Fault Zone, response spectra)
— Ss-4EW (Nagaoka Plain Western Rim Fault Zone, fault model method)
— S2
— Estimated ground motion on the free surface of base stratum at the time of the
Niigata-Chuetsu-Oki Earthquake

Fig. 22. Response spactra of the design basis ground motions.

On the basemat of reactor building	Unit 1	Unit 2	Unit 3	Unit 4	Unit 5	Unit 6	Unit 7
NCO Earthquake (observed values)	680	606	384	492	442	322	356
Ss Response acceleration	845	809	761	704	606	724	738

On the free surface of base stratum	Unit 1	Unit 2	Unit 3	Unit 4	Unit 5	Unit 6	Unit 7
The peak value of the design basis ground motion S_2	450						
The peak value of the design basis ground motion Ss	2,300				1,209		

The value represents the larger value among horizontal ones
(south-north and east-west). (Unit: Gal)

Fig. 23. Peak acceleration value of the design basis ground motions.